

Silicon quantum-dots-based optical probe for fluorometric detection of Cr⁶⁺ ions

Do Duc Tho^{1*}, Luyen Van Nam¹, Nguyen Thi Thanh Huyen¹, Pham Manh Hung¹, Pham Van Thang¹,
Truong Thi Ngoc Lien²,

¹Hanoi University of Science and Technology, 58 Le Thanh Nghi St., Hanoi, Vietnam

²Vietnam – Korea Institute of Science and Technology, Hi – tech Incubation and Training Centre,
Km29 Thang Long Boulevard, Hanoi, Vietnam

* Correspondence to Do Duc Tho <tho.doduc@hust.edu.vn>

(Received: 6 October 2021; Accepted: 9 November 2021)

Abstract. In this report, silicon quantum dots (SiQDs) with the NH₂ functional group were synthesized with the hydrothermal method. The as-prepared SiQDs exhibit a strong fluorescence emission peak at 441 nm when excited at 355 nm and are effectively quenched upon adding Cr⁶⁺ ions. Hence, SiQDs were used as an optical probe to detect Cr⁶⁺ ions in solutions. The crystal structure of SiQDs was characterized by using X-ray diffraction (XRD). The Fourier-transform infrared spectroscopy (FT-IR) was used to determine the linker groups on the SiQDs surface. The fluorescence spectroscopic technique with an excitation wavelength of 355 nm was used to quantify the Cr⁶⁺ ion concentration in the solutions in the range of 0.1–1000 μM. Competition from common coexisting ions, such as K⁺, Na⁺, Al³⁺, Zn²⁺, and Pb²⁺, was ignorable. The test with actual samples showed good linearity for the Cr⁶⁺ concentration range of 0.1–50 μM.

Keywords: Cr⁶⁺ ion, fluorometric detection, Si quantum dots, SiQDs, optical probe, hydrothermal method

1 Introduction

Over the past decades, the increasing toxicity of heavy metals has seriously affected the environment. One of those heavy metals is chromium, which exists in different oxidation states. Trivalent chromium (Cr³⁺) and hexavalent chromium (Cr⁶⁺) are primary oxidation states in the environment. Cr⁶⁺ ions have a stronger impact on human health and the environment than Cr³⁺ ions because of its high solubility, carcinogenicity, mutagenicity, and teratogenicity in biological systems [1]. While Cr⁶⁺ exists primarily as highly

soluble oxyanions [2], Cr³⁺ is less soluble and readily precipitates as Cr(OH)₃. Cr³⁺ has low toxicity and is considered an essential nutrient for many organisms [3]. In contrast, Cr⁶⁺ is 1000-fold more toxic than Cr³⁺ [4]. Nevertheless, the Cr⁶⁺ ion and other Cr⁶⁺ ion forms are used in different industries, including leather tanning, electroplating, painting, and metallurgy [1]. Therefore, chromium contamination has been reported in various industrial sites because of accidental leakages or improper disposal [6-9]. Hence, the determination of total chromium is crucial for environmental impact studies.

Recently, quantum dots (QDs) have attracted much attention because of their unique physical and optical properties, such as strong absorption, high quantum yield, fluorescence emission, availability for resizing by adding functional groups in the nanoscale, and high stability [10]. However, toxic inorganic precursors are commonly used in synthesizing traditional QDs and may harm various biological systems [11]. Among the quantum dots, those of silicon, semiconductor Si nanoparticles ranging from 1 to 10 nm, have attracted much attention in analytical science because of their advantages, such as inertness, nontoxicity, abundance, and low cost [12]. In addition, their highly efficient fluorescence makes them promising optical probes for various biomedical and biological applications [13].

In this paper, the silicon quantum dots (SiQDs) with NH_2 functional groups, synthesized with the hydrothermal method, were used as an optical probe for detecting Cr^{6+} ions in solutions via the fluorescence quenching mechanism. Their structure and fluorescence properties were also addressed.

2 Experimental

2.1 Synthesis of SiQDs solution

All reagents used in the experiments were purchased from Sigma-Aldrich in the analytical grade without further purification. First, 1 g of trisodium citrate (TSC) was completely dissolved in 30 mL of deionized water (DI) in a Teflon cup under magnetic stirring and aerated simultaneously with high-purity nitrogen to purge dissolved oxygen for 30 minutes. Next, 3 mL of 3-aminopropyl triethoxysilane (APTES) was added to the solution. The mixture was continuously stirred and aerated with nitrogen for five minutes. Afterwards, the Teflon cup was put in a stainless steel vessel, tightened, and covered

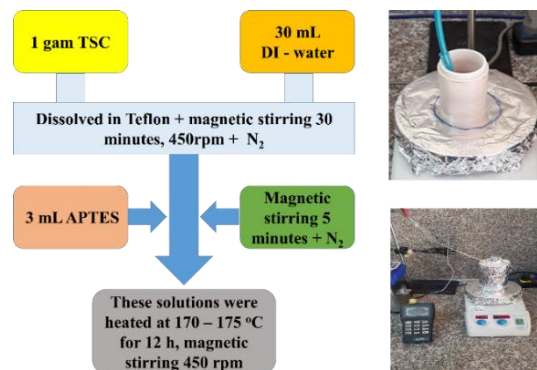


Fig. 1. Schematic illustration for stock SiQDs solution synthesis

with foil. The system was heated for 12 hours at 170 °C under magnetic stirring with a speed of 450 rpm. Finally, a SiQDs solution with yellowish colour was obtained. The synthesis schema of the stock SiQDs solution is shown in Fig. 1. From the obtained SiQDs solution, we prepared derivative SiQDs solutions for subsequent experiments by diluting it at the 1:300, 1:600, and 1:1200 (v/v) ratios. After dilution, these derivative SiQDs solutions strongly emitted a blue colour when excited with UV light of a 365 nm wavelength. The derivative SiQDs solution at the 1:600 dilution ratio was selected for the subsequent measurements.

2.2 Preparation of Cr^{6+} solutions

The 100 mM Cr^{6+} solution was obtained by dissolving 147.092 g potassium dichromate ($\text{K}_2\text{Cr}_2\text{O}_7$) in 10 mL of DI water and then used as the first stock solution. Firstly, the derivative stock solutions with a concentration of 0.1, 1, 10, and 100 mM were prepared by diluting the first stock solution with an appropriate volume of DI water. Secondly, the Cr^{6+} ion solutions of different final concentrations were also prepared by diluting a specific volume of appropriate derivative stock solutions with a relevant volume of DI water. The concentration of these final Cr^{6+} ion solutions is shown in the first column of Table 1.

Table 1. Volume of Cr⁶⁺ ion solutions (μL)

Final Solutions	Derivate Stock Solution 				DI H ₂ O
	Cr ⁶⁺ (100 mM)	Cr ⁶⁺ (10 mM)	Cr ⁶⁺ (1 mM)	Cr ⁶⁺ (0.1 mM)	
	0.01			100	900
	0.02			200	800
	0.05			500	500
	0.1				900
	1		100	100	900
	2		200		800
	2.5		250		750
	5		500		500
	6		600		400
	7		700		300
	8		800		200
	9		900		100
	10	100			900
	15	150			850
	20	200			800
	30	300			700
	40	400			600
	50	500			500
	60	600			400
	70	700			300
80	800			200	
90	900			100	
100	1000				

2.3 Preparation of actual samples

Some actual samples were taken from Van Phuc village, the To Lich river, and the Nguyen Lan river, and they were subjected to sedimentation for 12 hours. Then, they were transferred into 1 mL glass vessels and named VP1, VP2, VP3, TL1,

TL2, TL3, TL4, TL5, NL1, and NL2 according to where they were collected (Van Phuc village, the To Lich river, and the Nguyen Lan river). Afterwards, a solution containing Cr⁶⁺, K⁺, Na⁺, Al³⁺, Zn²⁺, and Pb²⁺ ions was dropped into each glass vessel. The obtained actual samples are shown in the first three columns of Table 2.

Table 2. Volume of wastewater samples (μL)

	Van Phuc village	To Lich river	Nguyen Lan river	Cr ⁶⁺ (5 mM)	Cr ⁶⁺ (100 mM)	K ⁺ (20 mM)	Na ⁺ (20 mM)	Al ³⁺ (20 mM)	Zn ²⁺ (20 mM)	Pb ²⁺ (20 mM)
VP1	1000									
VP2	940				10	10	20	10	10	
VP3	905				30	10	10	20	10	15
TL1		1000								
TL2		960		15		15	10			
TL3		945		20		10	15	10		
TL4		935			15	10	20	10	10	
TL5		885			35	20	10	20	10	20
NL1			1000							
NL2			965	15		10	10			

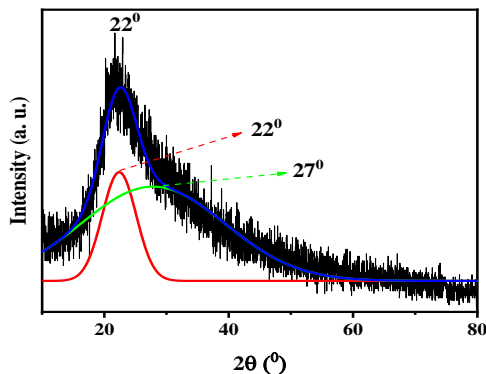
2.4 Instrumentation

The crystalline phase of the SiQDs was characterized by using X-ray diffraction (XRD) on an XRD Siemens D5005 diffractometer with Cu-K α radiation ($2\theta = 10\div 80^\circ$, step 0.02°). Fluorescence spectra were measured on a spectrofluorometer FL 3-22, Jobin Yvon-Spex, USA. FT-IR spectra were recorded with a wave number range of $375\text{--}4000\text{ cm}^{-1}$ on a Jasco 4600 Fourier-transform spectrophotometer. All the measurements were carried out at ambient temperature.

3 Results and discussions

The X-ray diffraction pattern of SiQDs is shown in Fig. 2. We can see that the broad diffraction peak at 22° is unclear and disturbed.

The deconvolution of the X-ray diffraction pattern reveals the presence of the peaks assigned to amorphous SiO₂ (at approximately 22° – the red

**Fig. 2.** XRD pattern and its deconvolution of SiQDs

curve) and crystal plane (111) of crystal Si (at approximately 28° – the green curve) [14]. The crystalline grain size calculated from the Scherrer formula for this crystal plane is 0.34 nm (green curve).

The absorption spectrum of SiQDs is presented in Fig. 3. A typical absorption band centred at about 236 nm can be attributed to the $\pi\text{--}\pi^*$ transitions of N-SiQDs bonds [15]. Fig. 4 displays the FT-IR spectra of SiQDs and APTES in

the ranges of 375–2000 cm^{-1} (Fig. 4a) and 2000–4000 cm^{-1} (Fig. 4b). The FT-IR spectrum of SiQDs reveals the existence of the C–H, O–Si–O, –NH₂, and Si–O–Si bonds in both APTES and SiQDs samples. The peak at 470 cm^{-1} is attributed to the bending vibrations of O–Si–O (14). Strong N–H bending vibrations at 1590 cm^{-1} and 3370 cm^{-1} (Fig. 4a, 4b, bottom) indicate the presence of the –NH₂ group on the SiQDs surface. Thanks to the presence of the –NH₂ group, SiQDs are well dispersed in water. Furthermore, the peak at 3370 cm^{-1} appears in the APTES spectrum (Fig. 4b, up) with a weaker intensity than the one in the SiQDs spectrum (Fig. 4b, bottom) because the vibration of the –NH₂ bond appears more clearly in SiQDs.

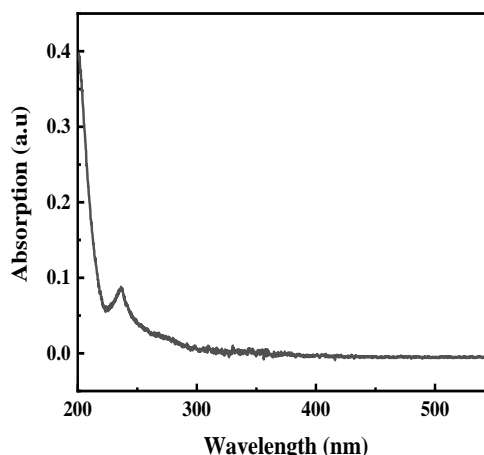


Fig. 3. XRD pattern and its deconvolution of SiQDs

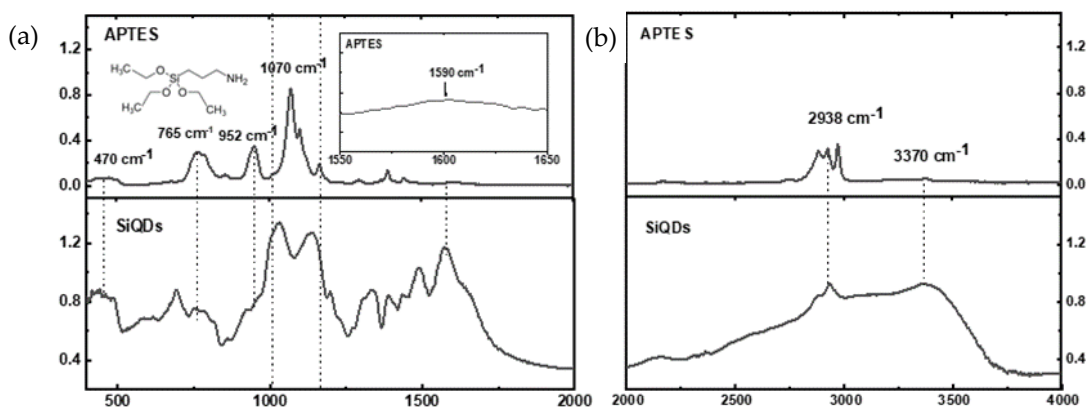


Fig. 4. FT-IR spectra of APTES and SiQDs in wavenumber ranges of 375–2000 (a) and 2000–4000 cm^{-1} (b)

Fig. 5a displays the excitation and fluorescence spectra of SiQDs, and Fig. 5b demonstrates the fluorescence spectra of SiQDs solution with different Cr⁶⁺ ion concentrations. The characteristic absorption peak at 355 nm reveals that the synthesized SiQDs are uniformly dispersed [16]. The maximal emission intensity of SiQDs is observed at 441 nm. Similarly, as shown in the inset of Fig. 5a, the SiQDs are transparent in daylight and emit intense blue colour under the illumination of UV irradiation at 365 nm. Furthermore, the stability of SiQDs is confirmed by the fluorescence spectra of SiQDs at different intervals. The as-synthesized SiQDs are stable even after two-month storage at –10 °C. In contrast, H₂O and other Cr⁶⁺ solutions emit

primarily at a wavelength of 396 nm. The emission peak at the 452 nm wavelength is weak or absent (Fig. 5b).

The qualitative result of Cr⁶⁺ ion detection is shown in Fig. 6. The colour images of the samples containing Cr⁶⁺ ion in the range of 1–1000 μM were taken under daylight (Fig. 6a) and UV light with a wavelength of 365 nm (Fig. 6b). Notably, the fluorescence intensity of the SiQDs solutions decreases remarkably with increasing Cr⁶⁺ concentration. The fluorescence spectra in Fig. 7 demonstrate that all peaks localize at the 441 nm wavelength. Their intensity decreases with increasing Cr⁶⁺ concentration, indicating that Cr⁶⁺ possibly forms complexes with SiQDs.

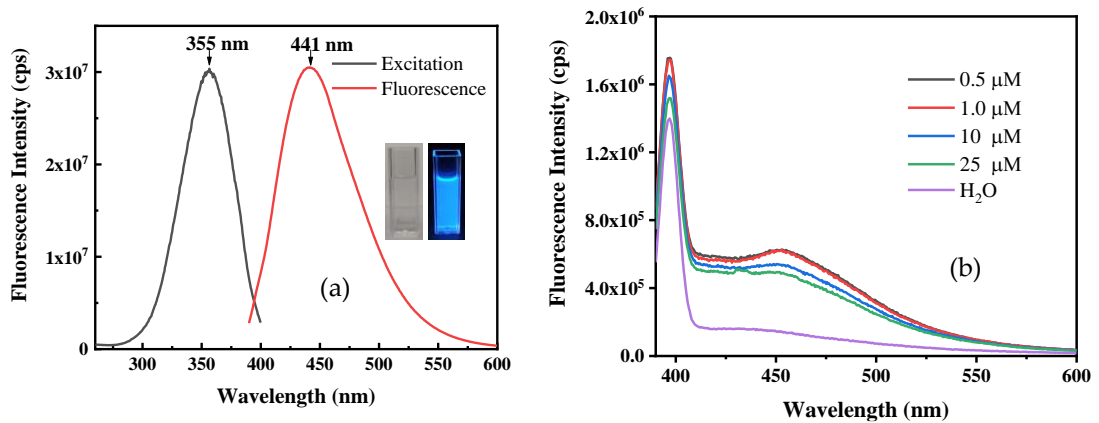


Fig. 5. Excitation and fluorescence spectra of SiQDs (a) and fluorescence spectra of added Cr⁶⁺ ion solutions (b)

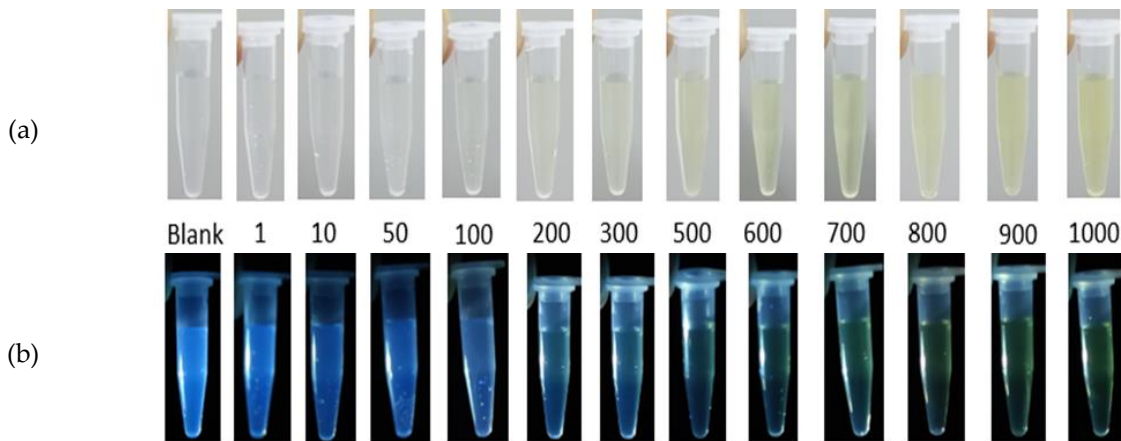


Fig. 6. Fluorescence of Cr⁶⁺ solutions corresponding to concentrations in the range of 1–1000 μM under daylight (a) and UV irradiation with wavelength of 365 nm (b)

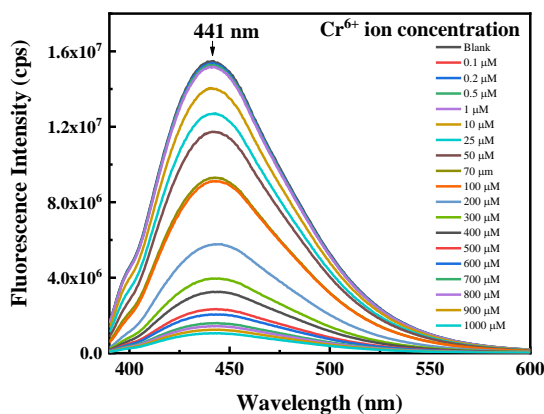


Fig. 7. Fluorescence spectra of SiQDs solutions (1:1200) with Cr⁶⁺ ion solutions with concentration in the range of 0.1–1000 μM

Under UV illumination (365 nm), electrons move from the valence band to the conduction band in SiQDs. Some of them might recombine with holes in the valence band and emit a photon. Others might combine with N atoms. Hence, the N atoms become more mobile. When the Cr⁶⁺ ions are present, the nitrogen atoms transfer these electrons to them, forming complexes between the SiQDs and the Cr⁶⁺ ions. Thus, the peak intensity in the fluorescence spectra of the SiQDs decreases with increasing Cr⁶⁺ ion concentration. The mechanism of the fluorescence quenching is shown in Fig. 8.

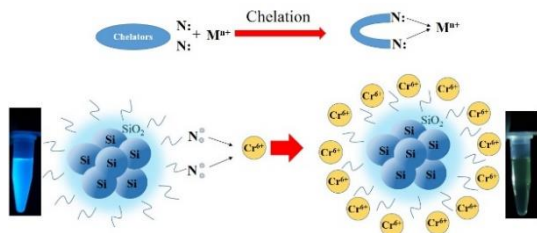


Fig. 8. Mechanism of the SiQDs fluorescence quenching

Fig. 9 illustrates the dependence of fluorescence intensity on Cr^{6+} ion concentration in the solutions of the SiQDs probes. It can be seen that the fluorescence intensity increases with the increasing concentration of the SiQDs. Probe 1:300 is the most sensitive, and probe 1:1200 reaches saturation rapidly. According to the linearity of the standard curve in the range of 0.1–50 μM , we chose probe 1:1200 for detecting Cr^{6+} ions in actual samples.

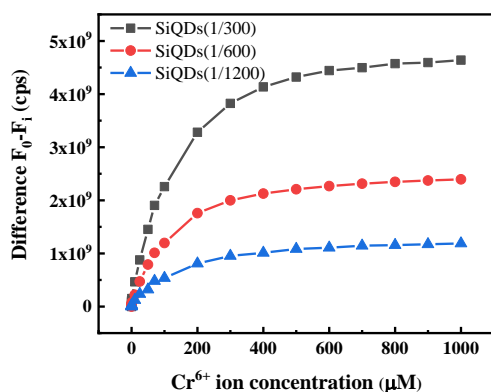


Fig. 9. Difference of emission intensities at 441 nm in the absence (F_0) and presence (F) of Cr^{6+} of different SiQDs probes added different concentrations of Cr^{6+} ion

Fig. 10 shows the selectivity of the SiQDs optical probe to Cr^{6+} , K^+ , Na^+ , Al^{3+} , Zn^{2+} , and Pb^{2+} in the solutions with a concentration of 200 μM . It can be noticed that the SiQDs optical probe reaches the best sensitivity to the Cr^{6+} ion.

Fig. 11 displays the fluorescence spectra of the actual samples. It is obvious that increasing the Cr^{6+} ion concentration leads to a decrease in the fluorescence signal in the VPs and Tls groups. The fluorescence intensity of the TL5 sample decreases substantially, corresponding to the most added Cr^{6+} amount. The calibration curve is linear

for Cr^{6+} ion concentrations ($R^2 = 0.998$) from 0.1 to 50 μM (Fig. 12). The actual and determined Cr^{6+} ion concentration is approximately the same (Tab. 3). Hence, the optical probe can detect the Cr^{6+} ion concentration in actual samples.

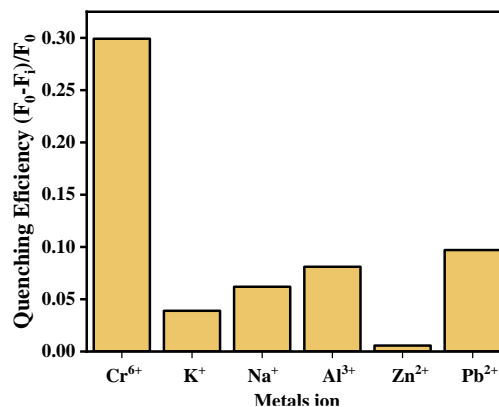


Fig. 10. The selectivity of SiQDs optical probe to Cr^{6+} ion

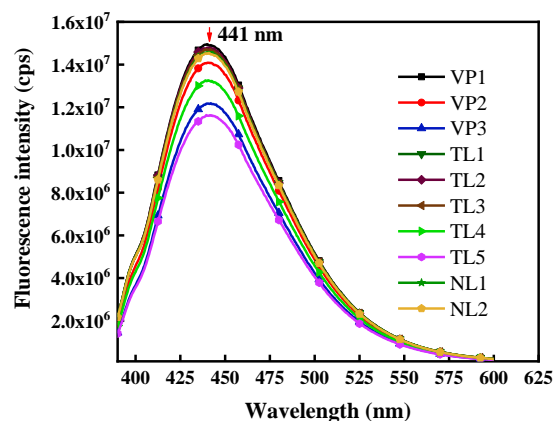


Fig. 11. Fluorescence spectra of the SiQDs optical probe for actual samples

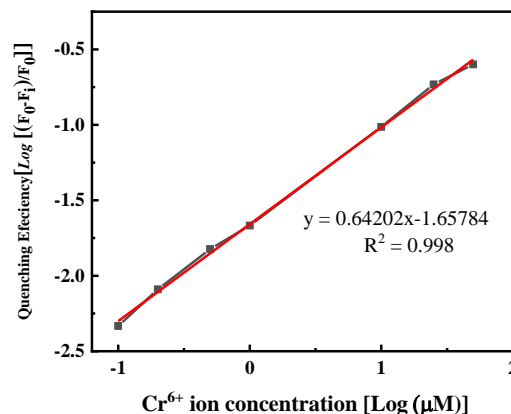


Fig. 12. Calibration curve of the changes in relative fluorescence intensity ($F_0 - F$)/ F_0 versus Cr^{6+} concentrations in logarithmic scale

Table 3. Comparison of actual and found Cr⁶⁺ ion concentration

Name	Cr ⁶⁺ ion conc. (actual) (μM)	(F ₀ - F _i)/F ₀	Cr ⁶⁺ ion conc. (found) (μM)
VP1	1.1	0.0235	1.1
VP2	11.4	0.0822	7.8
VP3	31.0	0.2102	33.7
TL1	2.0	0.0343	2.0
TL2	2.6	0.0317	1.7
TL3	2.9	0.0368	2.2
TL4	16.9	0.1372	17.3
TL5	36.8	0.2444	42.6
NL1	2.7	0.0421	2.7
NL2	3.4	0.0472	3.3

4 Conclusion

We successfully synthesized SiQDs with surface functionalization. The SiQDs optical probe exhibited high sensitivity towards Cr⁶⁺ ions and was used to detect and qualify actual samples. The method has good linearity in the range of 0.1–50 μM.

Funding statement

This research was financially supported by Hanoi University of Science and Technology under the project code T2020-PC-224.

References

- Dupont L, Guillon E. Removal of hexavalent chromium with a lignocellulosic substrate extracted from wheat bran. *Environ Sci Technol.* 2003;37:4235-41.
- Fendorf SE. Surface reactions of chromium in soils and waters. *Geoderma.* 1995;67:55-71.
- Pechova A, Pavlata L. Chromium as an essential nutrient: A review. *Vet Med (Praha).* 2007;52:1-18.
- Costa M. Potential hazards of hexavalent chromate in our drinking water. *Toxicol Appl Pharmacol.* 2003;188:1-5.
- Onchoke KK, Sasu SA. Determination of Hexavalent Chromium (Cr(VI)) Concentrations via Ion Chromatography and UV-Vis Spectrophotometry in Samples Collected from Nacogdoches Wastewater Treatment Plant, East Texas (USA). *Adv Environ Chem.* 2016;2016:1-10.
- Shrivastava R, Upreti RK, Chaturvedi UC. Various cells of the immune system and intestine differ in their capacity to reduce hexavalent chromium. *FEMS Immunol Med Microbiol.* 2003;38:65-70.
- Flury B, Eggenberger U, Mäder U. First results of operating and monitoring an innovative design of a permeable reactive barrier for the remediation of chromate contaminated groundwater. *Appl Geochemistry.* 2009;24:687-96.
- Ragosta M, Caggiano R, D'Emilio M, Macchiato M. Source origin and parameters influencing levels of heavy metals in TSP, in an industrial background area of Southern Italy. *Atmos Environ.* 2002;36:3071-87.
- Zazo JA, Paull JS, Jaffe PR. Influence of plants on the reduction of hexavalent chromium in wetland sediments. *Environ Pollut* 2008;156:29-35.
- Resch-Genger U, Grabolle M, Cavaliere-Jaricot S, Nitschke R, Nann T. Quantum dots versus organic dyes as fluorescent labels. *Nat Methods.* 2008;5:763–75.
- Lewinski N, Colvin V, Drezek R. Cytotoxicity of nanopartides. *Small.* 2008;4:26-49.
- Cheng X, McVey BFP, Robinson AB, Longatte G, O'Mara PB, Tan VTG, et al. Colloidal silicon quantum dots: from preparation to the modification of self-assembled monolayers for

- bioimaging and sensing applications. *Colloid Nanoparticles Biomed Appl* XII. 2017;10078: 100780O.
13. Phan LMT, Baek SH, Nguyen TP, Park KY, Ha S, Rafique R, et al. Synthesis of fluorescent silicon quantum dots for ultra-rapid and selective sensing of Cr(VI) ion and biomonitoring of cancer cells. *Mater Sci Eng C*. 2018;93:429-36.
 14. Terada S, Xin Y, Saitow KI. Cost-Effective Synthesis of Silicon Quantum Dots. *Chem Mater*. 2020;32:8382-92.
 15. Wang X, Yang Y, Huo D, Ji Z, Ma Y, Yang M, et al. A turn-on fluorescent nanoprobe based on N-doped silicon quantum dots for rapid determination of glyphosate. *Microchim Acta*. 2020; 187.
 16. Holmes JD, Ziegler KJ, Doty RC, Pell LE, Johnston KP, Korgel BA. Highly luminescent silicon nanocrystals with discrete optical transitions. *J Am Chem Soc*. 2001;123:3743-8.